Iranian Journal of Chemistry and Chemical Engineering (IJCCE)

Micromixing of non-Newtonian fluids in a passive micromixer with an inner eccentric cylindrical obstacle

Morteza Bayareh[1,*], Narges Jafari Ghahfarokhi[2]

[1]Department of Mechanical Engineering, Shahrekord University, Shahrekord, Iran

[2]Department of Mechanical Engineering, University of Isfahan, Isfahan, Iran

*m.bayareh@sku.ac.ir

Abstract

Micromixers have various applications in chemical, biological, and medical industries. Even though many liquids experience non-Newtonian behavior, a few investigators have examined their micromixing. In the present paper, the mixing performance of shear-thinning non-Newtonian liquids in a passive micromixer with an inner eccentric cylindrical obstacle is assessed numerically by employing the Carreau-Yasuda model. The time evolution of the mixing process is analyzed and the influences of the power-law index, inlet velocity, and relaxation time on the mixing index are evaluated. It is demonstrated that the mixing index is improved with time and reduces with the inlet velocity. The pressure drop is a descending function of inlet velocity. Besides, the diffusion coefficient does not have a considerable impact on the mixing index. The results reveal that the mixing index of shear-thinning fluids is larger than that of a Newtonian one under the same conditions. For instance, MI = 63.7% and 33.1% when n = 0.1 and 1, respectively.

Keywords: *Microfluidics, Passive micromixer, Mixing index, Non-Newtonian fluids.*

1. Introduction

Advances in technology have led scientists to examine substances in small dimensions such as nano and micro. Microfluidics is an interdisciplinary science that emerges from a broad range of scientific disciplines, including medicine, chemistry, physics, biology, metallurgy, biotechnology, nanotechnology, etc. [1-3]. Micromixers are essential components of Lab-on-a-Chip (LoC) systems because mixing is a fundamental process in many chemical reactions. Chemical applications in this regard include crystallization, extraction, polymerization, and organic synthesis, applications including enzyme assays, biological screening, such as selective sorting of biomolecules or cells, bioassay processes, including cell separation, cell lysis, decomposition and DNA analysis, and protein folding [4].

The amount of Reynolds number is very low in microchannels. Therefore, molecular diffusion plays a major role in the mixing process due to the lack of turbulence and inertia forces. To achieve a proper mixing quality, a long mixing length or long residence time is required, which is not possible in most practical applications. In such cases, the use of passive micromixers with complex geometries or active ones is recommended. Micromixers are categorized into two groups: active and passive. Active micromixers utilize an external force, such as the electroosmotic [5], magnetic [6], acoustic [7], etc. to augment the mixing index. However, in passive micromixers, the fluids are mixed without external actuators and perform under the influence of the specific geometry of their microchannel. Passive micromixers have always been more attractive due to lower costs than active ones. Numerous designs have been presented for passive micromixers, including T-shaped [8-10], Y-shaped [11], and more complex ones [12]. For example, Bothe et al. [8] assessed the mixing quality of a simple T-shaped micromixer and recognized three flow regimes based on the average velocity. They revealed that an engulfment regime may lead to high mixing quality. Rasouli et al. [9] evaluated the mixing index in a simple T-shaped micromixer with obstacles and demonstrated that the presence of obstacles in the chamber improves the mixing index by about 43% at low Reynolds numbers. Arshad and Kim [10] examined the effect of the Reynolds number on the mixing process of a sinusoidal mixer and reached a mixing efficiency of about 80%. Lee et al. [11] presented a 100 mm-wide zigzag microchannel integrating with a Y-shaped micromixer. They assessed the influence of the periodic step on the mixing quality experimentally and indicated that the mixing efficiency can be improved from 65% to 83.8% when the aspect ratio is augmented from 1 to 8 at Re = 0.26. Ansari et al. [12] investigated various T-shaped micromixers and compared their performance with the conventional one. They found that a simple T-shaped micromixer is not suitable for mixing, because an increase in the Reynolds number results in a negative effect on the mixing performance. Bhagat et al. [13] examined the mixing process in a micromixer with obstacles at low Reynolds numbers numerically and experimentally. Diamond-shaped obstacles with different arrangements were used for splitting and recombining the two flows,

indicating that the mixing quality can be improved while the amount of pressure drop is kept low. Cortelezzi et al. [14] evaluated a micromixer for biomedical applications numerically and achieved a high mixing efficiency. By assessing the dimensionless numbers, such as Reynolds, Peclet, and Strouhal numbers, it was concluded that an increase in the frequency improves the amount of mixing index.

The examination of micromixing of Newtonian and non-Newtonian fluids has been performed up to now. Recent numerical and experimental investigations have aimed to propose efficient micromixers that can be fabricated easily with the minimum cost. For instance, Zhou et al. [15] considered spiral and serpentine micromixers to examine the impact of the Dean vortex on the mass transfer during micromixing. It was found that vortical flow generated in serpentine micromixer leads to a higher mixing index than spiral one. The performance of two micromixers with fan-shaped obstacles was analyzed by Jin et al. [16] and Jafari Ghahfarokhi et al. [17]. Jin et al. [16] proposed the micromixer and reached a mixing efficiency of > 94% for Reynolds numbers ranging from 0.5 to 100. They employed the DoE algorithm to optimize the micromixer. Jafari Ghahfarokhi et al. [17] utilized seven machine learning algorithms to optimize another type of micromixer with fan-shaped obstacles. They proposed two correlations for mixing index and pressure drop based on effective variables and demonstrated that the mixing index is improved by enhancing inlet velocity, obstacle radius, and number of mixing units.

Micromixing of non-Newtonian liquids has been considered by a few investigators. They mostly evaluated the mixing efficiency of non-Newtonian fluids in the presence of the electric field. For example, Usefian et al. [18] analyzed an electro-osmotic micromixer consisting of two eccentric cylinders to compare the mixing quality of Newtonian and non-Newtonian fluids. The inner cylinder rotated with various angular velocities. It was concluded that the mixing degree is an ascending function of frequency, angular velocity, and voltage and a descending function of inlet velocity. Yang et al. [19] employed an electric actuator to improve the mixing quality of polyacrylamide solutions as non-Newtonian fluids by utilizing the Oldroyd-B constitutive equation. They revealed that the mixing index is augmented by reducing the obstacle zeta potential. Considering the spiral passive micromixer, Tokas et al. [20] numerically assessed the micromixing of non-Newtonian fluid blood and reached a mixing index of 97%. It was demonstrated that spiral geometry significantly improves the mixing quality in comparison with a T-shaped channel.

The present work aims to examine the mixing efficiency of two non-Newtonian liquids in the passive micromixer proposed by Cortelezzi et al. [14] (Fig. 1). The time evolution of the mixing process and the effect of the power-law index, relaxation time, and inlet velocity on the mixing index are analyzed. This paper is organized as follows: the governing equations are presented in section 2. In section 3, the numerical method and grid study are described and the results are discussed in section 4. Eventually, concluding remarks are presented in section 5.

2. Governing equations

Initially, the reference geometry is studied based on the one used by Cortelezzi et al. [14] (Fig. 1). A non-Newtonian fluid with different concentrations is injected into the inlets 1, 2, and 3 at the same velocity. The governing equations for an incompressible non-Newtonian fluid are continuity and momentum equations that can be expressed as follows:

$$\nabla \cdot \vec{V}_f = 0 \tag{1}$$

$$\rho_f \left(\frac{\partial \vec{V}_f}{\partial t} + \vec{V}_f \cdot \nabla \vec{V}_f \right) = -\nabla P + \nabla \cdot \vec{\tau} \tag{2}$$

where $\vec{V}_f$ is the fluid velocity vector, p is the pressure, and ρ_f is the density. $\vec{\tau} = \mu \vec{\dot{\gamma}}$ denotes the shear stress tensor. The dynamic viscosity has a constant value for Newtonian fluids. The dynamic viscosity of non-Newtonian fluids can be stated by utilizing the Carreau-Yasuda model:

$$\mu = \mu_\infty + (\mu_0 - \mu_\infty)\left[1 + (\lambda \vec{\dot{\gamma}})^2\right]^{\frac{n-1}{2}} \tag{3}$$

where μ_0 is the zero shear rate viscosity, μ_∞ is an infinite shear rate viscosity, and λ is a time constant (relaxation time). Besides, n is the power-law index that accounts for the shear-thinning behavior of the model (n < 1) in the present simulations. The constants of the model for human blood are: μ_0 = 0.056 $Pa{\cdot}s$, μ_∞ = 0.0035 $Pa{\cdot}s$, λ = 3.313 and n = 0.3568. The strain rate tensor $\dot{\gamma}$ is defined as:

$$\vec{\dot{\gamma}} = \left(\nabla \vec{V}_f\right) + \left(\nabla \vec{V}_f\right)^T \tag{4}$$

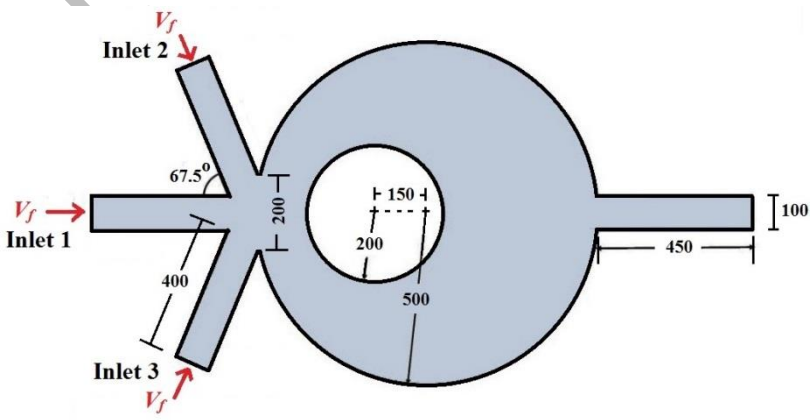

Fig. 1. Schematic of the micromixer (all dimensions are in micrometer).

The convection-diffusion equation for species is also defined as follows:

$$\nabla \cdot \vec{J} = 0 \tag{5}$$

where $\vec{J}$ is the mass flux that is defined as:

$$\vec{J} = -D\nabla\vec{C} + \vec{V}_f\vec{C} \tag{6}$$

where $\vec{C}$ is the local concentration and D indicates the diffusion coefficient.

The boundary conditions in the concentration field are as follows: $C = 1$ for the inlet 1 of microchannel (stream 1), and $C = 0$ for the inlets 2 and 3 (stream 2). In addition, no flux boundary is imposed on the other boundaries:

$$\vec{n} \cdot \left(-D\nabla\vec{C} + \vec{V}_f\vec{C}\right) = 0 \tag{7}$$

Also, the no-slip and no-penetration boundary conditions are used on the entire internal surface of the micromixer.

Mixing index, MI, is calculated to quantify the performance of the micromixer:

$$MI = 1 - \sqrt{\frac{\iint (c - \bar{c})^2 \, dA}{A.\bar{c}(c_{max} - \bar{c})}} \tag{8}$$

The mixing index is the average concentration at the cross-section of the outlet channel. A is the outlet channel cross-section, and c_{max} is the maximum sample concentration in the microchannel. According to Eq. 8, MI = 0 and 1 represent no mixing and complete mixing, respectively.

3. Numerical method and grid study

The governing equations for laminar incompressible flow are solved by a finite-element method utilizing COMSOL Multiphysics software. The computational domain is discretized by unstructured triangular elements. The P2+P2 algorithm is employed to couple velocity and pressure fields. Fig. 2a shows the results of the grid independence test for the present simulations when n = 0.3568. Five grid resolutions, i.e., normal, fine, finer, extra fine, and extremely fine, are employed to study the grid study. Fig. 2a demonstrates that the grid resolutions of 98456 (extra fine) and 146224 (extremely fine) lead to the same amount of mixing index. Hence, the grid with 98456 elements is used for further simulations. Besides, Fig. 2b illustrates a view of the fine grid to clearly experience the triangular elements and grid refinement in particular zones of the computational domain.

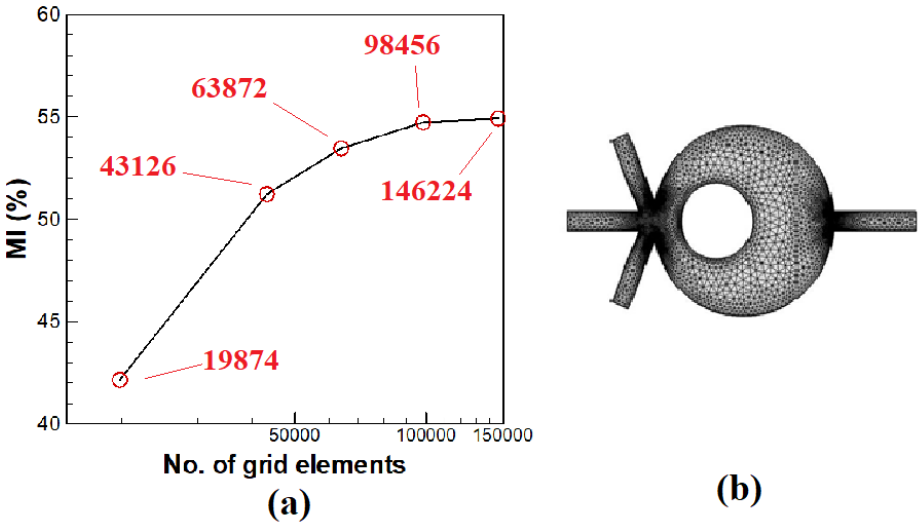

Fig. 2. (a) Mixing index at the outlet of micromixer for different grid resolutions when V_f = 0.05 m/s and t = 10 s. (b) A view of the fine grid.

4. Results

4.1. Validation

To verify the present simulations, the numerical results are compared against the experimental results of Zivkovic et al. [21] who studied the efficient mixing in a Y-shaped micromixer. Fig. 3 demonstrates the mixing efficiency along the micro-channel and shows that the present results are in very good agreement with the experimental ones. It should be mentioned that the experimental results correspond to the time-dependent condition (t = 40s).

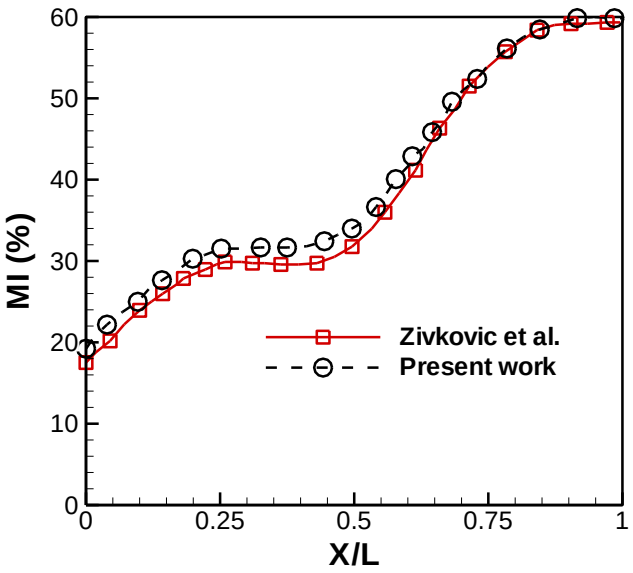

Fig. 3. Mixing index along the microchannel for V_f = 190 μm/s at t = 40 s.

4.2. Effect of power-law index

The most important application of mixing in biotechnology is the mixing of non-Newtonian fluids such as blood. This section deals with the mixing of non-Newtonian fluids with various power-law indices. Several non-Newtonian models are commonly used for the simulation of non-Newtonian fluids: Power-law, Carreau-Yasuda, Casson, etc. In the present work, the Carreau-Yasuda model is employed to evaluate the non-Newtonian behavior of two fluids during the mixing process. It should be mentioned that this model is an appropriate one for the modeling of shear-thinning fluids. Three constants of the model for human blood in Eq. 3 are μ_0 = 0.056 $Pa \cdot s$, μ_∞ = 0.0035 $Pa \cdot s$, λ = 3.313, and n = 0.3568. Hence, these properties are selected for the present simulations except when the influences of the power-law index are evaluated. Fig. 4a depicts the distribution of concentration contours in the micromixer for different amounts of power-law index. This figure qualitatively indicates that the mixing degree is improved by reducing the value of *n*. In other words, two non-Newtonian fluids can be mixed better by more deviation from Newtonian behavior. For instance, MI = 63.7% and 33.1% when *n* = 0.1 and 1, respectively.

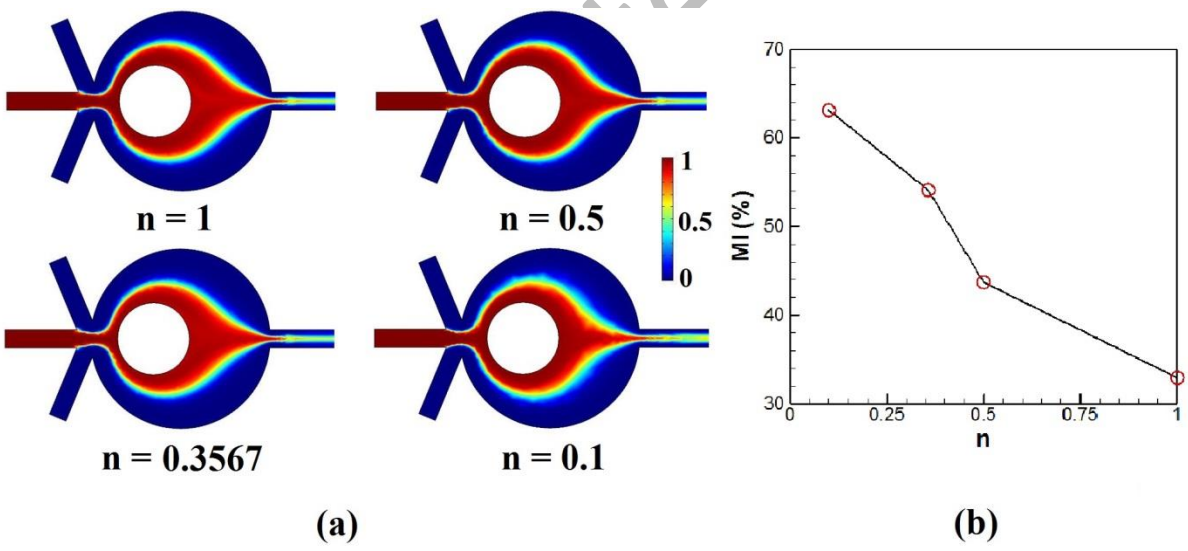

Fig. 4. Effect of power-law index: (a) Concentration distribution throughout the micromixer. (b) Mixing index at the outlet of the micromixer when V_f = 0.05 m/s at t = 10s.

4.3. Time evolution of the mixing process

Fig. 5a demonstrates the concentration fields along the micromixer for different times, indicating that the mixing quality does not vary during 10s < t < 40s qualitatively. Fig. 5b quantitatively indicates that the mixing index is enhanced firstly and then remains constant

when the time rises so that the mixing index at the outlet changes from 9.2% at 2s to 55.1% at 40s. In other words, after a specific time, when the time is enhanced, the mixing quality does not change. It should be pointed out that the real-time impact is different from the residence time. The residence time in passive micromixers with complex geometry, such as spiral ones or the ones with a large number of obstacles, is high, resulting in high amounts of mixing index and pressure drop.

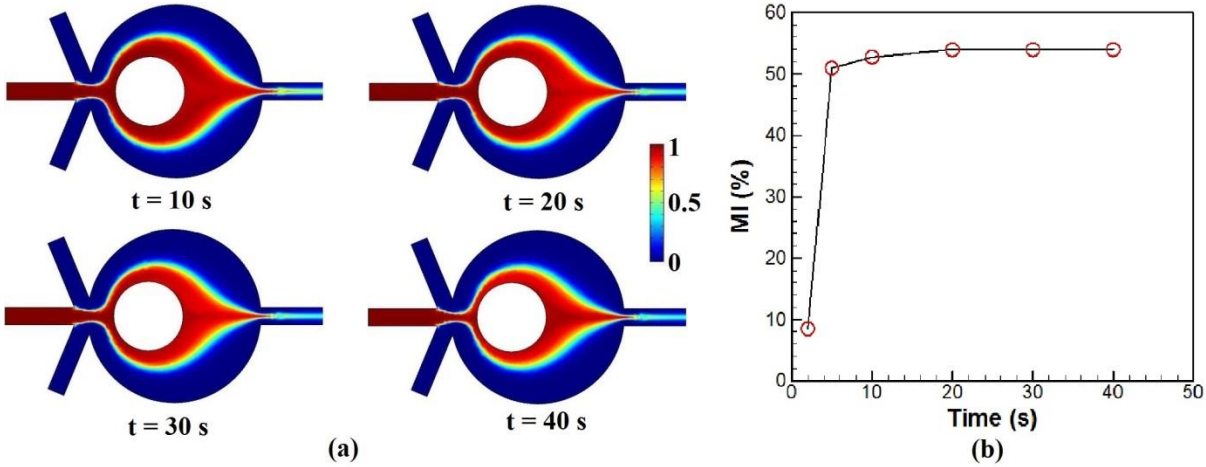

Fig. 4. (a) Time evolution of concentration profile throughout the microchannel. (b) Mixing index at the outlet of the micromixer at different times when n = 0.3568 and $V_f = 0.05\ m/s$.

4.4. Effect of inlet velocity

In this section, the effect of inlet velocity is considered to find the relation between mixing efficiency and velocity variations. The concentration distribution throughout the micromixer is presented in Fig. 6a for different inlet velocities at t = 10s, showing an improvement in the mixing quality by reducing the inlet velocity. The amount of the mixing index at the outlet of the microchannel is plotted as a function of inlet velocity in Fig. 6b. The results demonstrate that an enhancement in the inlet velocity declines the mixing index. The amount of mixing index is about 68.33% for V_f = 0.025 m/s. By doubling the velocity, the mixing index decreases to 54.1%. The downward trend in the mixing index continues and at V_f = 0.2 m/s, it reaches 44.84%. In other words, the mixing index reduces by about 34% when V_f augments from 0.025 m/s to 0.2 m/s. As expected, the value of pressure drop is reduced by increasing the inlet velocity for this range of Reynolds number. It should be pointed out that molecular diffusion plays a major role in the micromixing process when the inlet flow rate (Reynolds number) is low. By enhancing the amount of inlet flow rate, the value of MI may be improved depending on the occurrence of chaotic advection. In other words, an optimum point may be observed for a greater range of Reynolds numbers.

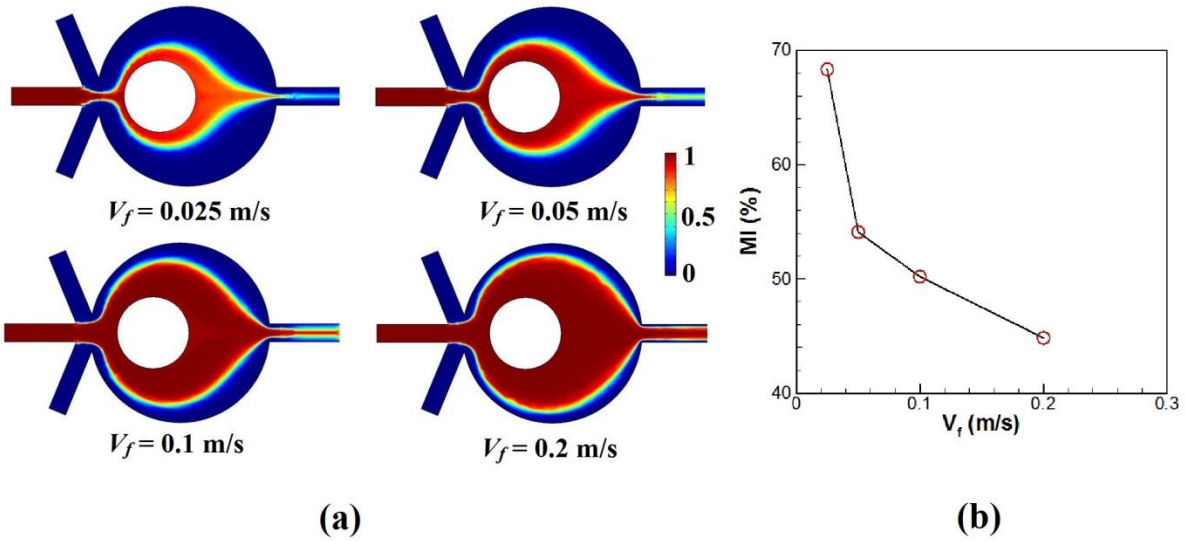

Fig. 6. Effect of inlet velocity: (a) Concentration distribution throughout the micromixer. (b) Mixing index at the outlet of the micromixer when n = 0.3568 and t = 10s

4.5. Effect of diffusion coefficient

The amount of diffusion coefficient depends on the fluid employed in real applications. It has been found that the impact of the diffusion coefficient on velocity, pressure, and mixing quality of Newtonian fluids is small because this parameter does not affect the velocity distribution or pressure perturbation. For instance, the diffusion coefficient of water and blood at 25 °C is about 2.3×10^{-9} m^2/s and 1.1×10^{-9}, respectively. Fig. 7 illustrates the variations of MI by changing the value of the diffusion coefficient ranging from 10^{-8} to 10^{-14} when n = 0.3568, V_f = 0.05 m/s, and t = 10s. It is found that the amount of MI is improved by enhancing the diffusion coefficient slightly. For example, MI = 54.5% and 53.46% for 10^{-8} to 10^{-14}, respectively.

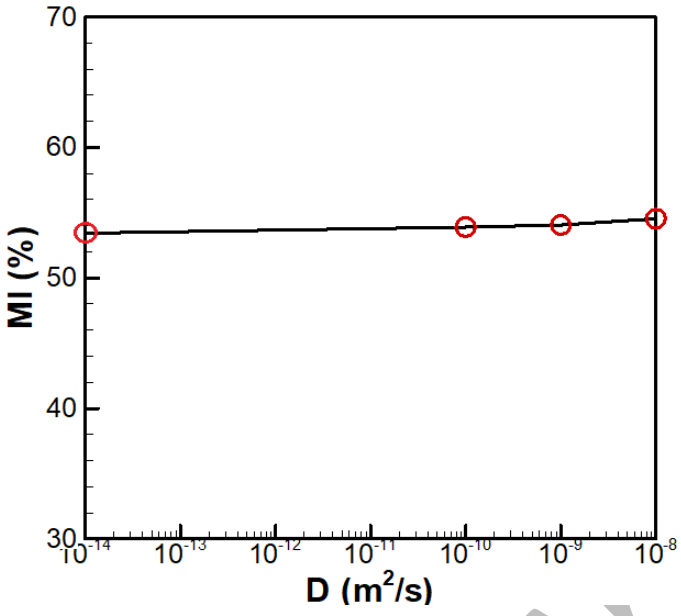

Fig. 7. Effect of diffusion coefficient on mixing index at the outlet of the micromixer when n = 0.3568, V_f = 0.05 m/s, and t = 10s.

5. Conclusions

In the present paper, the effect of different parameters on the mixing index in a micromixer is studied by considering non-Newtonian fluids. It is revealed that the mixing process is enhanced first and then remains constant with time. The results indicate that the mixing index is a descending function of inlet velocity and power-law index. For instance, MI = 63.7% and 33.1% when n = 0.1 and 1, respectively, and MI = 68.33% for V_f = 0.025 m/s. By doubling the velocity, the mixing index decreases to 54.1%. It is demonstrated that the diffusion coefficient impact can be neglected in the mixing of non-Newtonian fluids. For future works, it is recommended to assess the micromixing of shear-thickening non-Newtonian fluids for a broader range of inlet velocity.

Nomenclature

C	Fluid concentration (mol/m^3)	x, y	Coordinates (m)
D	Diffusion coefficient (m^2/s)	**Greek symbols**	
$\vec{J}$	Mass flux (kg/m^{2}s)	$\vec{\tau}$	Shear stress tensor (Pa)
MI	Mixing index	ρ	Density (kg/m^3)
n	Power-law index	μ	Dynamic viscosity (Pa.s)
P	Pressure (Pa)	λ	Time constant (s)

t	Time (s)	$\vec{\dot{\gamma}}$	Strain rate tensor (1/s)
$\vec{V}$	Velocity vector (m/s)		

References

[1] Bayareh M., An updated review on particle separation in passive microfluidic devices, *Chemical Engineering and Processing-Process Intensification*, 153: 107984 (2020).

[2] Bayareh M., Nazemi Ashani M., Usefian A., Active and passive micromixers: A comprehensive review, *Chemical Engineering and Processing - Process Intensification*, 147: 107771 (2020).

[3] Hessel V, Löwe H, Schönfeld F., Micromixers—a review on passive and active mixing principles, *Chemical Engineering Science*, 60 (8–9): 2479-2501 (2005).

[4] Mohammadali R., Bayareh M., Ahmadi Nadooshan A., Numerical investigation on the effects of cell deformability and DLD microfluidic device geometric parameters on the isolation of circulating tumor cells, *Iranian Journal of Chemistry and Chemical Engineering*, doi: 10.30492/ijcce.2023.1988916.5849.

[5] Usefian A., Bayareh M., Numerical and experimental study on mixing performance of a novel electro-osmotic micro-mixer, *Meccanica*, 54: 1149–1162 (2019).

[6] Ghahfarokhi N.J., Bayareh M., Numerical study of a novel spiral-type micromixer for low Reynolds number regime, *Korea-Aust. Rheol. J.*, 33: 333–342 (2021).

[7] Ghorbani Kharaji Z., Kalantar V., Bayareh M., Acoustic sharp-edge-based micromixer: a numerical study, *Chem. Pap.*, 76: 1721–1738 (2022)

[8] Bothe D, Carsten S, Warnecke H.J., Fluid mixing in a T-shaped micro-mixer, *Chemical Engineering Science*, 61(9): 2950-2958 (2006).

[9] Rasouli M.R., Abouei Mehrizi A., Lashkaripour A., Numerical Study on Low Reynolds Mixing of T-Shaped Micro-Mixers with Obstacles, *Trans. Phenom. Nano Micro Scales*, 3(2): 68-76 (2015).

[10] Arshad A., Kim K.Y., Performance Evaluation of Three Types of Passive Micromixer With Convergent-Divergent Sinusoidal Walls, *Journal of Marine Science and Technology-Taiwan*, 22(6): 680-686 (2014).

[11] Lee C.Y., Lin C.H., Fu L.M., Encyclopedia of Microfluidics and Nanofluidics, *Encyclopedia of Microfluidics and Nanofluidics*, (1): 1-12 (2013).

[12] Ansari M., Kim K., Anwar K., Kim S., Vortex micro T-mixer with non-aligned inputs, *Chemical Engineering Journal*, 181-182: 846-850 (2012).

[13] Bhagat A.A., Erik T., Peterson K., Papautsky I., A passive planar micromixer with obstructions for mixing at low Reynolds numbers, *Journal of Micromechannics and Microengineering*, 17: 1017-1024 (2007).

[14] Cortelezzi L., Ferrari S., Dubini G., A scalable active micro-mixer for biomedical applications, *Microfluid Nanofluid*, 21: 31 (2017).

[15] Zhou D., Qin L., Yue J., Yang A., Jiang Z., Zheng S., Numerical and experimental investigations of spiral and serpentine micromixers over a wide Reynolds number range, *International Journal of Heat and Mass Transfer*, 212: 124273 (2023).

[16] Jin H., Wang D., Liu P., Chang Y., Chen Y., Sun Y., Xu Y., Qian X., Zhu W., Design and scale-up of a superb micromixer with fan-shaped obstacles for synthesis of Dolutegravir intermediate, *Chemical Engineering and Processing - Process Intensification*, 195: 109638 (2024).

[17] Jafari Ghahfarokhi N., Bayareh M., Nourbakhsh A., Baghoolizadeh M., Optimization of a novel micromixer with fan-shaped obstacles, *Chem. Pap.*, https://doi.org/10.1007/s11696-024-03380-y.

[18] Usefian A., Bayareh M., Shateri A. Taheri N., Numerical study of electro-osmotic micro-mixing of Newtonian and non-Newtonian fluids, *J Braz. Soc. Mech. Sci. Eng.*, 41: 238 (2019).

[19] Yang J., Chen Y., Du C., Guan X., Li J., Numerical simulation of electroosmotic mixing of non-Newtonian fluids in a micromixer with zeta potential heterogeneity, *Chemical Engineering and Processing - Process Intensification*, 186: 109339 (2023).

[20] Tokas S., Zunaid M., Ansari M.A., Non-Newtonian fluid mixing in a Three-Dimensional spiral passive micromixer, *Materials Today: Proceedings*, 47: 3947-3952 (2021).

[21] Zivkovic V., Ridge N., Biggs M.J., Experimental study of efficient mixing in a micro-fluidized bed, *Applied Thermal Engineering*, 127: 1642-1649 (2017).